SSN 0965-5441, Petroleum Chemistry, 2022, Vol. 62, No. 5, pp. 515–525. © The Author(s), 2022. This article is an open access publication.
Russian Text © The Author(s), 2022, published in Neftekhimiya, 2022, Vol. 62, No. 3, pp. 375–386.

Equilibrium Composition of Products Formed by Non-catalytic Conversion of Hydrocarbons

V. I. Savchenko[a,b], Ya. S. Zimin[a,b,*], E. Busillo[c], A. V. Nikitin[a,b], I. V. Sedov[a,b], and V. S. Arutyunov[a,b]

[a] *Institute of Problems of Chemical Physics, Russian Academy of Sciences, Chernogolovka, 142432 Russia*
[b] *Federal Research Center of Chemical Physics, Russian Academy of Sciences, Moscow, 119991 Russia*
[c] *Gubkin Russian State University of Oil and Gas (National Research University), Moscow, 119991 Russia*
**e-mail: iaroslaw.zimin@gmail.com*

Received February 8, 2022; revised March 10, 2022; accepted April 4, 2022

Abstract—The kinetic patterns of the attainment of the equilibrium product composition in non-catalytic processes of partial oxidation and of steam and carbon dioxide reforming of hydrocarbons in the temperature range 1400–1800 K, characteristic of these processes, were analyzed. The need for such analysis is caused by the rapidly increasing consumption of natural gas as a chemical feedstock and by growing attention to environmental problems, in particular, to a decrease in CO_2 emissions or to partial CO_2 utilization. The forward and reverse water gas shift reactions (WGSRs) play an important role in approach to the equilibrium product composition in these processes. Analysis has shown that the elementary reactions characteristic of forward and reverse WGSRs start to play a significant role long before the equilibrium in the system is attained. Already in the intermediate steps of the process, the distribution of the major reaction products, H_2, CO, H_2O, and CO_2, almost corresponds to the equilibrium value of $K_t = ([H_2][CO_2])/([CO][H_2O])$, close to the WGSR equilibrium constant K_{eq}, and further conversion of the products occurs at K_t values close to K_{eq}.

Keywords: natural gas, partial oxidation, steam reforming, carbon dioxide reforming, equilibrium product composition, water gas shift reaction, equilibrium constant

DOI: 10.1134/S0965544122050048

In the most important non-catalytic processes of the conversion of natural gas and separate hydrocarbons, such as their partial oxidation and steam and carbon dioxide reforming, the major final products are CO, H_2, CO_2, and H_2O, and their distribution in the course of the process and upon its completion is an important process characteristic. Although processes of non-catalytic conversion of hydrocarbons are mainly controlled by kinetic factors, at the high temperature required for their occurrence the product distribution tends to the equilibrium composition. Similar composition of products is also characteristic of the well-studied reaction of steam reforming of CO (water gas shift reaction, WGSR):

$$CO + H_2O \leftrightarrow CO_2 + H_2,\ \Delta H^\circ_{298} = -41\ \text{kJ/mol}, \quad (1)$$

in which the equilibrium distribution of the components is determined by the equilibrium constant (Eq. (2)).

$$K_{eq} = \frac{[CO_2][H_2]}{[CO][H_2O]}. \quad (2)$$

Calculation of K_{eq} for WGSR at various temperatures attracted researchers' attention for a long time. Haber and Richard in 1904 [1] present the formula for K_{eq}, obtained as early as the XIX century:

$$\log K_{eq} = -2232/T - 0.08463\log T - 0.002203T + \text{const}. \quad (3)$$

As assumed previously [1], in partial oxidation of rich methane–oxygen mixtures the equilibrium is attained already in the flame. However, this conclusion was based on the results of the experiments in which the product samples from the flame were taken using samplers made of platinum, which catalyzes reaction (1). Today, refined calculation formulas or tables with the K_{eq} values at different temperatures are available.

Table 1. Equilibrium constants K_{eq} of the steam reforming of CO in the temperature interval 1200–1800 K

Temperature, K	1200	1300	1400	1500	1600	1700	1800
K_{eq}	0.727	0.566	0.459	0.385	0.331	0.291	0.260
K_{eq} (3)	0.733	0.572	0.466	0.393	0.339	0.300	0.269

The reverse water gas shift reaction (rWGSR) acquires importance today in connection with increasing use of natural gas as a gas-chemical feedstock and growing attention to environmental problems, in particular, with strengthening of requirements to reduction of the CO_2 emission or its partial utilization, because the reaction of CO_2 with H_2 may become one of the ways to solve this problem [2]. Along with catalytic processes in which the WGSR equilibrium is attained relatively rapidly [3], non-catalytic processes also attract attention today. In these processes, the equilibrium is attained in considerably longer time and not in all the cases. Therefore, it is necessary to analyze the kinetic patterns of gas-phase non-catalytic forward and reverse reactions of steam CO conversion in the temperature range 1400–1800 K, characteristic of non-catalytic gas-chemical processes, in particular, the kinetics of the attainment of the equilibrium in non-catalytic processes of partial oxidation and of steam and carbon dioxide reforming of hydrocarbons. That is the subject of this paper.

EXPERIMENTAL

Thermodynamic analysis of the product distribution for such non-catalytic reactions as WGSR, partial oxidation of hydrocarbons, and their steam and carbon dioxide reforming at 1400–1800 K was performed using the Terra program [4]. For the kinetic calculations, we used the mechanism of the oxidation of light hydrocarbons [5, 6], based on the experimental data on oxidation of light hydrocarbons in impact tubes and rapid compression machines at T = 770–1580 K, P = 101–5050 kPa, and oxygen/alkane ratio of 1.0–4.0, i.e., under the conditions close to those of this study. Its reliability was proved by modeling the production of acetylene by partial oxidation of methane [7] under the conditions similar to those of this study, and also of our experiments on selective oxycracking of casinghead gases [8]. In both cases, good agreement between the experimental data and modeling results was demonstrated.

Modeling was performed in the Chemical Workbench program environment for the model of a flow-through reactor [9] under isothermal conditions. Although methane conversion processes are not isothermal under real conditions, we chose this mode to simplify the analysis for modeling. The nonisothermal character of the process exerts no essential effect on its overall physicochemical pattern, affecting largely only its time characteristics [10]. Along with significant simplification, modeling under isothermal conditions was also appropriate because of the fact that, according to the results of preliminary studies, the maximal conversion of the main intermediate C_2H_2 and the maximal yield of hydrogen and syngas are reached at a high temperature. Therefore, to ensure the maximal syngas yield, it is desirable to preserve the high temperature, maintaining it on the level as close to the initial temperature as possible.

Detailed kinetic modeling allows us to follow the kinetics of the variation of reactant and product concentrations in the course of the process and the sequence of changes occurring in the system on its way to the thermodynamic equilibrium.

RESULTS AND DISCUSSION

Thermodynamic Analysis of the Equilibrium in the C–H–O System

The equilibrium distribution of WGSR components is determined by the equilibrium constant (Eq. (2)).

Refined calculation formulas analogous to Eq. (3) or tables with K_{eq} values at various temperatures are available today (see, e.g., [3]).

Table 1 presents the results of calculating K_{eq} for the WGSR reaction in the temperature interval 1200–1800 K from the equilibrium concentrations of H_2, CO, H_2O, and CO_2, estimated using the Terra program [4], and by Eq. (3).

For this temperature interval, K_{eq} can also be determined by a simple but sufficiently accurate formula [11]:

$$K_{eq} = 0.0305e^{3811/T}, \text{ or } \ln K_{eq} = 3811/T - 3.49. \quad (4)$$

Table 2. Equilibrium composition of products formed by thermal conversion of CH_4

Concentration, mol/mol CH_4	Temperature, K								
	500	700	800	900	1000	1100	1300	1400	1500
CH_4	0.990	0.832	0.607	0.337	0.152	0.066	0.016	0.010	0.005
H_2	0.020	0.335	0.786	1.327	1.697	1.868	1.964	1.980	1.990
C_{solid}	0.010	0.168	0.393	0.664	0.848	0.934	0.984	0.990	0.995

The elemental base of the steam reforming of CO consists of C, H, and O atoms, and the most stable gaseous compounds at 1400–1800 K are CO, H_2O, H_2, and CO_2, between which these atoms are virtually exclusively distributed at equilibrium. The equilibrium concentrations of other gaseous compounds that could contain these atoms, e.g., methane, in this temperature interval are too low (Table 2) to noticeably influence the distribution described by the forward and reverse reactions of steam reforming of CO.

High-temperature non-catalytic processes of partial oxidation of rich methane (hydrocarbon)–oxygen mixtures and of steam and carbon dioxide reforming of hydrocarbons, and also some other processes also involve reactions with the participation of three elements, C, H, and O. The equilibrium gas mixtures formed by these processes at temperatures higher than 1400 K, similarly to the steam reforming of CO, can contain as major products only CO, H_2O, H_2, and CO_2.

Because the product distribution at equilibrium is independent of the reaction pathway and is fully determined by the initial ratio of the C, H, and O atoms, the equilibrium distribution for the reactions under consideration, as well as for the steam reforming of CO, can be expressed via elements:

$$C + nH + mO \rightarrow \text{Products}. \quad (5)$$

That is, instead of considering the equilibrium for each of the reactions occurring in the system, we can consider the general relationships of the equilibrium in system (5), where n and m vary in a definite range.

For the steam reforming of CO, $n = 2$ and $m = 2$.

For the carbon dioxide reforming of C_1–C_4 hydrocarbons (from CH_4 to C_4H_2) at $m = 1$, n varies from 0.25 to 2. For example, for the reaction

$$CH_4 + CO_2 \rightarrow \text{Products}, \quad (6)$$

this initial state will be 2C + 4H + 2O, or, per mole of C,

$$C + 2H + O\ (n = 2). \quad (7)$$

For the reaction

$$C_4H_2 + 4CO_2 \rightarrow \text{Products}, \quad (8)$$

the initial state will be 8C + 2H + 8O, or, per mole of C,

$$C + 0.25H + O\ (n = 0.25). \quad (9)$$

For the steam reforming of C_1–C_4 hydrocarbons at $m = 1$, n varies from 2.5 to 6, because for the reaction

$$CH_4 + H_2O \rightarrow \text{Products} \quad (10)$$

the initial state will be

$$C + 6H + O\ (n = 6). \quad (11)$$

For the reaction

$$C_4H_2 + 4H_2O \rightarrow \text{Products}, \quad (12)$$

the initial state will be 4C + 10H + 4O, or, per mole of C,

$$C + 2.5H + O\ (n = 2.5). \quad (13)$$

In Table 3, we present the results of calculating the equilibrium yield of products in steam and carbon dioxide reforming of C_1–C_4 hydrocarbons per mole of C at n from 0.25 to 6.0, temperatures of 1200–1800 K, and a pressure of 0.1 MPa. As seen from Table 3, at 1400–1800 K the equilibrium yield of CO and H_2 virtually corresponds to the stoichiometry of the reaction of the corresponding hydrocarbons with H_2O or CO_2. Such components as H_2O, CO_2, and CH_4 are present in trace amounts. At temperatures below 1600 K, C_{solid} (graphite in our calculations) appears in the products; its yield is the higher, the lower is n.

For partial oxidation of methane,

$$CH_4 + mO \rightarrow \text{Products}, \quad (14)$$

Table 3. Equilibrium yields of products of the reaction C + *n*H + O → Products per mole of C at 1200–1800 K and a pressure of 0.1 MPa

Yield, mol/mol C	Temperature, K							
	1200	1400	1600	1800	1200	1400	1600	1800
	n = 0.25				*n* = 2.0			
CO	0.9649	0.9965	0.9994	0.9998	0.9815	0.9964	0.9993	0.9996
H_2	0.1218	0.1245	0.1248	0.1249	0.9769	0.9937	0.9984	0.9990
CO_2	0.0162	0.0015	0.0003	0.0001	0.0055	0.0009	0.0001	<0.0001
H_2O	0.0028	0.0004	0.0001	<0.0001	0.0075	0.0019	0.0004	0.0003
CH_4	0.0002	0.0001	<0.0001	<0.0001	0.0078	0.0022	0.0005	0.0002
C_{solid}	0.0187	0.0019	0.0003	<0.0001	0.0052	0.0006	–	–
H_2/CO	0.126	0.125	0.125	0.125	1.00	1.00	1.00	1.00
K'_{eq}	0.73	0.46	0.33	0.26	0.73	0.46	0.33	0.26
	n = 2.5				*n* = 6.0			
CO	0.9788	0.9962	0.9989	0.9995	0.9658	0.9936	0.9983	0.9992
H_2	1.2187	1.2419	1.2476	1.2488	2.9197	2.9837	2.9952	2.9975
CO_2	0.0057	0.0008	0.0002	0.0001	0.0055	0.0008	0.0001	0.0001
H_2O	0.0097	0.0022	0.0007	0.0003	0.0231	0.0049	0.0016	0.0007
CH_4	0.0108	0.0029	0.0008	0.0003	0.0286	0.0057	0.0016	0.0006
C_{solid}	0.0047	–	–	–	–	–	–	–
H_2/CO	1.245	1.247	1.249	1.249	3.023	3.003	3.000	3.000
K'_{eq}	0.73	0.46	0.33	0.27	0.26	0.33	0.46	0.73

m varies usually from ~1.1 to 1.5 ($m = 2\psi$, where ψ is the $O_2 : CH_4$ molar ratio).

Data on the equilibrium yield of products of reaction (14) or reaction

$$C + 4H + mO \rightarrow \text{Products}$$

per mole of C at 1200–1800 K and a pressure of 0.1 MPa are given in Table 4.

As follows from Table 4, with an increase in *m* the yield of products of deep methane oxidation, H_2O and CO_2, increases, and the yield of CO and H_2 correspondingly decreases. The H_2/CO ratio decreases simultaneously. In the temperature range under consideration, there is no C_{solid} at equilibrium.

In Tables 3 and 4, we also present the values of $K'_{eq} = ([H_2]_{eq}[CO_2]_{eq})/([CO]_{eq}[H_2O]_{eq})$, calculated from the data on the distribution of component yields at equilibrium; for all the reactions under consideration, these values at a given temperature are equal and coincide with K_{eq} for the steam reforming of CO at the same temperature. Because the data on K_{eq} for this reaction are presented in the literature most completely, they can be used for calculating the equilibrium in other reactions involving the same elements at temperatures higher than 1400 K, in particular, for non-catalytic reactions of partial oxidation and steam and carbon dioxide reforming.

Therefore, for the reaction

$$C + nH + mO \rightarrow x_{eq}O + u_{eq}CO_2 + y_{eq}H_2 + z_{eq}H_2O, \quad (15)$$

where x_{eq}, u_{eq}, y_{eq}, and z_{eq} are the component yields at equilibrium, these quantities can be determined from the material balance for each element (three equations) and from the fourth equation characterizing the relationship between the concentrations under the preset conditions at equilibrium:

$$([H_2]_{eq}[CO_2]_{eq})/([CO]_{eq}[H_2O]_{eq}) = K'_{eq} = K_{eq}. \quad (16)$$

The balance equations for the elements are as follows:

$$\text{for C, } x_{eq} + u_{eq} = 1; \quad (17)$$

$$\text{for H, } y_{eq} + z_{eq} = 0.5n; \quad (18)$$

$$\text{for O, } x_{eq} + 2u_{eq} + z_{eq} = m, \quad (19)$$

and the equation for the equilibrium constant is

Table 4. Equilibrium yields of products of the reaction C + 4H + *m*O → Products per mole of C at 1200–1800 K and a pressure of 0.1 MPa

Yield, mol/mol C	Temperature, K							
	1200	1400	1600	1800	1200	1400	1600	1800
	m = 1.1				*m* = 1.3			
CO	0.9677	0.9808	0.9854	0.9881	0.9168	0.9408	0.9540	0.9622
H_2	1.9152	1.9186	1.9145	1.9114	1.7787	1.7590	1.7459	1.7374
CO_2	0.0280	0.0190	0.0146	0.0119	0.0821	0.0592	0.0460	0.0378
H_2O	0.0762	0.0811	0.0855	0.0881	0.2191	0.2409	0.2540	0.2622
CH_4	0.0043	0.0002	<0.0001	–	0.0011	<0.0001	–	–
C_{solid}	–	–	–	–	–	–	–	–
H_2/CO	1.979	1.956	1.943	1.934	1.940	1.870	1.830	1.806
K'_{eq}	0.727	0.458	0.332	0.261	0.727	0.459	0.331	0.260
	m = 1.5							
CO	0.8611	0.8977	0.9193	0.9329				
H_2	1.6369	1.6023	1.5807	1.5668				
CO_2	0.1384	0.1023	0.0807	0.0671				
H_2O	0.3621	0.3977	0.4193	0.4329				
CH_4	0.0005	<0.0001	–	–				
C_{solid}	–	–	–	–				
H_2/CO	1.901	1.785	1.719	1.680				
K'_{eq}	0.726	0.459	0.331	0.260				

$$K'_{eq} = (u_{eq}y_{eq})/(x_{eq}z_{eq}). \quad (20)$$

For non-catalytic processes in the temperature interval 1400–1800 K, K'_{eq} can be determined by formula (4) for steam reforming of CO:

$$K'_{eq} = K_{eq} = 0.0305e^{3811/T}. \quad (21)$$

The solution of the system of four equations (17)–(20) with respect to x_{eq}, u_{eq}, y_{eq}, and z_{eq} gives the sought-for values of the equilibrium yield of each product at a given temperature and given values of *n* and *m*.

It should be noted that the reactions involving three elements C, H, and O, whose equilibrium products are CO, H_2O, H_2, and CO_2, include not only the above-considered four processes, but also the reactions of thermal pyrolysis and cracking of alcohols, ethers, esters, ketones, aldehydes, organic acids, carbohydrates, etc. At equilibrium, the distribution of the products of these reactions, described by formula (16), also corresponds to the WGSR equilibrium constant. Furthermore, the equilibrium mixture of products of methane oxidation with a stoichiometric amount of oxygen, $CH_4 + 2O_2$ (*n* = 4, *m* = 4), in the temperature interval 1200–1800 K contains not only CO_2 and H_2O, but also low concentrations of CO and H_2, and the equilibrium product distribution corresponds to formula (16).

Critical Temperature of the Appearance of C_{solid} in Equilibrium Products

All the processes under consideration are characterized by a critical temperature at which C_{solid} appears among equilibrium products. Figure 1 shows how the temperature at which a noticeable amount (0.01 mol %) of C_{solid} appears among equilibrium products in partial oxidation of rich methane–oxygen mixtures depends on the molar ratio $\psi = O_2 : CH_4$ [12].

As follows from Fig. 1, $\psi = 0.5$ is the boundary value at which it is still possible to determine the temperature boundary above which the syngas production is not accompanied by carbon black formation. At $\psi < 0.5$, because of the oxygen deficiency, thermal conversion of methane and CO always occurs, and C_{solid} is present as an equilibrium component throughout the temperature interval. Even a minor increase in ψ over the boundary $\psi = 0.5$ leads to a sharp decrease in the temperature below which C_{solid} is formed as one of the products. For

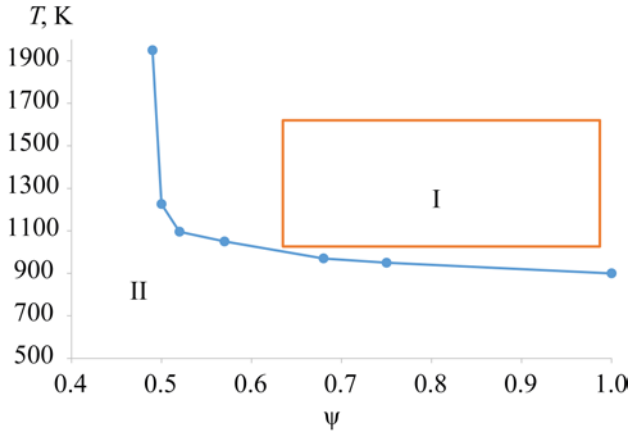

Fig. 1. Temperature at which C_{solid} appears among equilibrium products as a function of the $O_2 : CH_4$ molar ratio. The region of operation temperatures and ratios ψ at which the matrix conversion can be performed is conventionally shown by a rectangle.

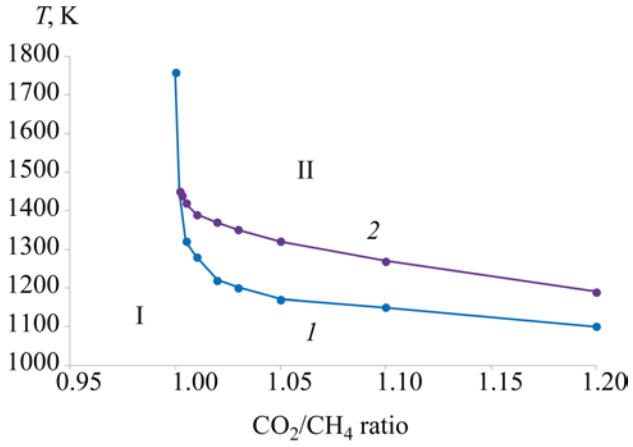

Fig. 2. Temperature at which C_{solid} appears among equilibrium products as a function of the CO_2/CH_4 ratio for the carbon dioxide reforming of methane. Pressure, atm: (*1*) 1 and (*2*) 2.

example, whereas at ψ = 0.5 the calculated temperature below which the carbon black formation starts (T_{cr} of carbon black formation) is ~1226 K, already at ψ = 0.52 it is more than 100 K lower, ~1096 K. The appearance of C_{solid} as one of the products in the system is preceded by the appearance of equilibrium products and by a gradual increase in the methane concentration with decreasing temperature.

As follows from Fig. 2, two characteristic regions can be conventionally distinguished: the first region at ψ > 0.5 and temperatures above 1000–1200 K (depending on ψ), when there is no C_{solid} in the system (I), and the second region (II) in which this component is present. The interval of the operation temperatures and values of ψ at which it is appropriate to perform partial oxidation of rich methane–oxygen mixtures falls into region I. In this region, virtually complete conversion of oxygen and methane is reached at equilibrium. Calculations also show that this region is characterized by significant effect of ψ and weak effect of temperature on the equilibrium hydrogen yield (it slightly decreases with increasing temperature at ψ > 0.5). The equilibrium yield of hydrogen reaches a maximum at ψ = 0.5 and does not change with a further decrease in ψ, coinciding with the equilibrium yield of hydrogen in thermal conversion of methane, $CH_4 \rightarrow C_{solid} + 2H_2$, i.e., at ψ = 0.

For the carbon dioxide reforming of methane (1), the calculated temperature at which C_{solid} appears in the equilibrium products as a function of the CO_2/CH_4 ratio at P = 1 atm is plotted in Fig. 2 (curve *1*). With an increase in the pressure, the temperature at which C_{solid} appears in the equilibrium products increases, so that the curve for P = 10 atm lies higher (curve *2*).

As seen from Fig. 2, with a decrease in the CO_2/CH_4 ratio T_{cr} increases; at the CO_2/CH_4 ratio slightly lower than unity, T_{cr} of carbon black formation sharply increases, so that carbon black will be formed at any practically relevant temperature (because of the deficiency of oxygen from CO_2 molecules for complete methane conversion and appearance of unchanged methane in the system). Region I in which the reaction is accompanied by the carbon black formation lies below line 1 or 2 (depending on pressure), and region II in which no carbon black is formed lies above this line.

The steam reforming of methane at $H_2O : CH_4 \geq 1$ occurs without formation of C_{solid} by-product [13].

Kinetics of Non-catalytic Processes of Hydrocarbon Conversion and WGSR at 1400–1800 K

Kinetics of forward and reverse non-catalytic WGSR. High conversion rate of CO and H_2O to H_2 and CO_2 for the forward reaction of steam reforming of CO (1) is reached at low temperatures. Owing to large practical role of this reaction in catalytic processes, which are performed, as a rule, at temperatures lower than 873 K, the catalytic version of this process became

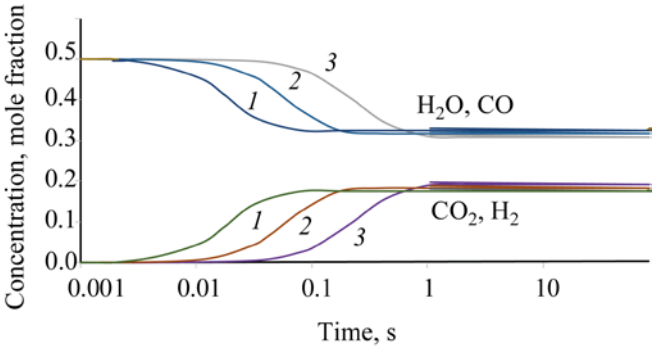

Fig 3. Variation of the gas mixture composition in non-catalytic steam reforming of CO under isothermal conditions. H_2O/CO = 1 : 1. Temperature, K: (*1*) 1700, (*2*) 1600, and (*3*) 1500.

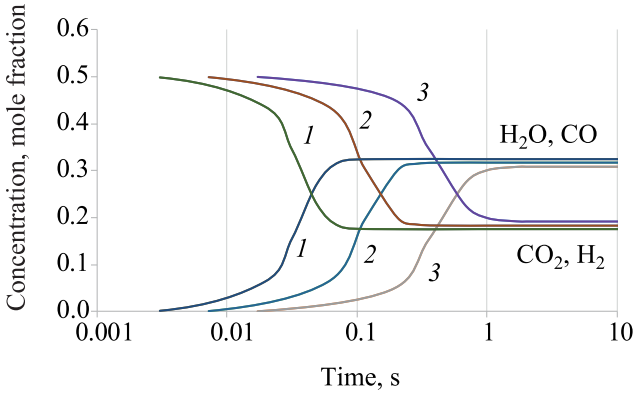

Fig. 4. Variation of the gas mixture composition in the course of non-catalytic reverse reaction of steam reforming of CO under isothermal conditions. CO_2/H_2 = 1 : 1. Temperature, K: (*1*) 1700, (*2*) 1600, and (*3*) 1500.

a subject of active research [3, 14]. Kinetic studies of the forward and reverse non-catalytic WGSR under these conditions became topical recently in connection with the interest in high-temperature non-catalytic processes for light hydrocarbon conversion. Bustamante et al. [15, 16] made an analytical review of data on the WGSR kinetics at elevated temperatures. A kinetic study of the high-temperature (1070–1134 K) WGSR in an empty quartz reactor and in a quartz reactor packed with quartz particles has shown that, at low conversion, the power expression for the reaction rate corresponded to the Bradford mechanism and was pressure-independent.

Bradford [17] suggested a simple gas-phase mechanism for the steam reforming of CO, presented below; for the forward reaction, it is the chain reaction mechanism. Reaction (22) ensures the chain initiation in the reaction of H_2O with any molecule in the gas phase (denoted as M). Reactions (23) and (24) are chain propagation reactions, whereas reaction (25) is a chain termination reaction.

$$H_2O + M \xrightarrow{k_1} H + OH + M, \quad (22)$$

$$CO + OH \underset{k_{-2}}{\overset{k_2}{\longleftrightarrow}} H + CO_2, \quad (23)$$

$$H_2O + H \underset{k_{-3}}{\overset{k_3}{\longleftrightarrow}} OH + H_2, \quad (24)$$

$$H + OH + M \xrightarrow{k_{-1}} M + H_2O. \quad (25)$$

In the approximation of steady-state concentration of chain carriers H and OH under the conditions of low conversion, the rate equation will be as follows:

$$r = \frac{d[CO_2]}{dt} = \left[\frac{k_1}{k_{-1}}k_2k_3\right]^{0.5}[CO]^{0.5}[H_2O], \quad (26)$$

$$k = \left[\frac{k_1}{k_{-1}}k_2k_3\right]^{0.5}, \quad (27)$$

$$r = \frac{d[CO_2]}{dt} = k[CO]^{0.5}[H_2O]. \quad (28)$$

Similarly, for the high-temperature inverse reaction of steam reforming of CO,

$$H_2 + M \xrightarrow{k_1} 2H + M, \quad (29)$$

$$H + CO_2 \underset{k_{-2}}{\overset{k_2}{\longleftrightarrow}} CO + OH, \quad (30)$$

$$OH + H_2 \underset{k_{-3}}{\overset{k_3}{\longleftrightarrow}} H_2O + H, \quad (31)$$

$$M + 2H \xrightarrow{k_{-1}} M + H_2 \quad (32)$$

and under the conditions of low conversion the rate equation will be as follows:

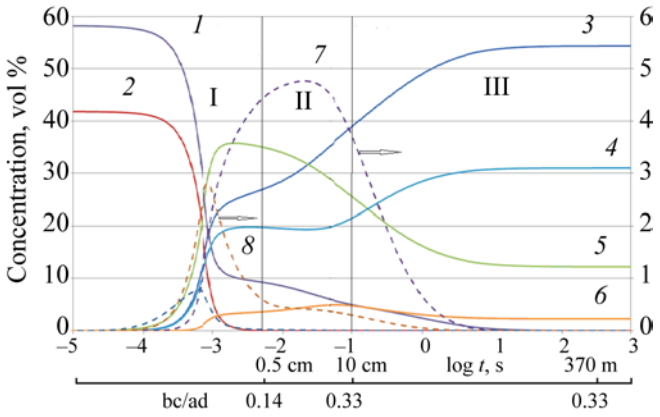

Fig. 5. Kinetics of variation of component concentrations in partial oxidation of methane in the isothermal mode at the volume ratio $O_2/CH_4 = 0.72 : 1$ and 1600 K: (*1*) CH_4, (*2*) O_2, (*3*) H_2, (*4*) CO, (*5*) H_2O, (*6*) CO_2, (*7*) C_2H_2, and (*8*) C_2H_4. bc/ad = $([CO_2][H_2])/([CO][H_2O])$.

$$r = \frac{d[\mathrm{CO}]}{dt} = \left[\frac{k_1}{k_{-1}}\right]^{0.5} k_2 [\mathrm{H_2}]^{0.5} [\mathrm{CO_2}] \qquad (33)$$

or

$$r = \frac{d[\mathrm{CO}]}{dt} = k [\mathrm{H_2}]^{0.5} [\mathrm{CO_2}]. \qquad (34)$$

For any value of the conversion, in accordance with the Bradford mechanism, the rate of the steam reforming of CO is described by the equation

$$r = \frac{d[\mathrm{CO}]}{dt} = k_2 [\mathrm{CO_2}][\mathrm{H}] - k_{-2} [\mathrm{CO}][\mathrm{OH}]. \qquad (35)$$

It has been shown that the kinetic description of the reaction with a more detailed set of elementary reactions and components used in modern programs for kinetic modeling of the oxidative methane conversion gives the results almost identical to the Bradford mechanism [16].

In [10], we modeled the kinetics of the steam reforming of CO at 1600 K. The results of modeling in a wider temperature interval are shown in Fig. 3; they demonstrate shortening of the induction period of this reaction with increasing temperature.

The kinetic modeling of the reverse non-catalytic WGSR at 1500–1700 K (Fig. 4) shows that this reaction also has an appreciable induction period, which decreases with increasing temperature.

Thus, the results of kinetic modeling show that both the forward and reverse reactions of steam reforming of CO have an induction period and that the equilibrium is attained rapidly within 0.1–1 s. The induction period of the forward and reverse reactions can be appreciably reduced by introducing certain compounds, e.g., C_2H_6.

Kinetics of the Attainment of the Equilibrium under the Conditions of Partial Oxidation and of Steam and Carbon Dioxide reforming of Methane

Partial oxidation of methane. As we showed previously by kinetic modeling [18], three steps can be distinguished in homogeneous partial oxidation of methane (Fig. 5).

The initial step of fast reactions involving oxygen (I) (flame zone) completes in a very short time (at 1600 K, about 5×10^{-3} s) with virtually complete oxygen conversion and formation of such major products as CO, H_2, H_2O, C_2H_4, and C_2H_2. The gas mixture containing these components plus unchanged methane arrives at the post-flame zone in which further transformations of the mixture components occur at temperatures of approximately 1600 K. The time at which the oxygen conversion becomes 99.8% can be conventionally considered as the time of completion of the first process step.

Then, in steps II and III, slower reactions occur without oxygen. In these steps, the H_2O vapor becomes an active converting agent. Its amount in this zone decreases by 15–20%. Whereas at the end of the flame zone $K_t = ([CO_2][H_2])/([CO][H_2O])$ is far from K'_{eq} at this temperature (Fig. 6), with the progress of the reactions in the post-flame zone (II), at times of ~0.1 s (at 1600 K), it becomes equal to K_{eq} and remains unchanged up to complete conversion of the unchanged methane and formed acetylene in zone III, i.e., under the conditions when the system as a whole is yet far from the equilibrium.

Figure 6 shows the variation of the quantity $K_t = ([CO_2][H_2])/([CO][H_2O])$ in the course of partial oxidation of methane at 1600 K (curve *4*). The same figure shows the variation of K_t when performing the partial oxidation of methane under the same conditions but with the addition of CO_2 (curves *1–3*) and H_2O (curves *5–7*).

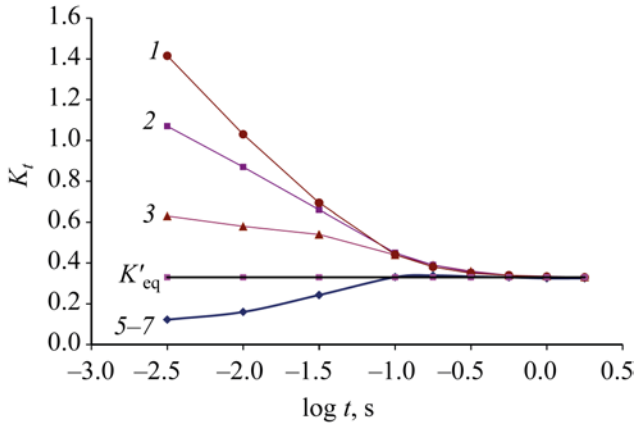

Fig. 6. Variation of the quantity $K_t = ([CO_2][H_2])/([CO][H_2O])$ in the course of (*4*) partial oxidation of methane at 1600 K and partial oxidation of methane with the addition of (*1–3*) CO_2 and (*5–7*) H_2O. $CO_2 : CH_4$ ratio: (*1*) 1.5 : 1, (*2*) 1 : 1, and (*3*) 0.5 : 1; $H_2O : CH_4$ ratio: (*5*) 0.5 : 1, (*6*) 1 : 1, and (*7*) 1.5 : 1.

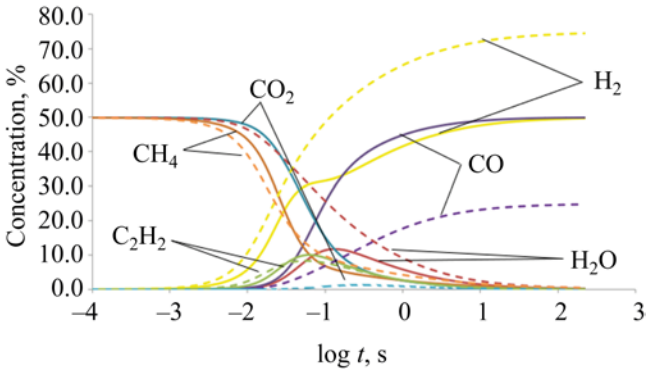

Fig. 7. Kinetics of carbon dioxide (solid lines) and steam (dashed lines) conversion of methane under isothermal conditions at CH_4/CO_2 = 1 : 1 and CH_4/H_2O = 1 : 1. T = 1600 K [11].

As can be seen, in partial oxidation of methane at 1600 K, $K_t = ([CO_2][H_2])/([CO][H_2O])$ at the end of the flame zone is lower than $K'_{eq} = K_{eq} = 0.33$, which suggests that the reaction equilibrium in this case is attained via forward reaction of the steam reforming of CO. When performing the process with the addition of H_2O, the equilibrium is attained similarly.

When performing the partial oxidation of methane with the addition of CO_2, the values of $K_t = ([CO_2][H_2])/([CO][H_2O])$ at $\log t \le -2.5$ and $[CO_2] : [CH_4] > 0.5$ significantly exceed the equilibrium constant of reaction (17), so that reverse reaction of the steam reforming of CO becomes possible under these conditions. Such dependence of $K_t = ([CO_2][H_2])/([CO][H_2O])$ on the $[CO_2] : [CH_4]$ ratio suggests that, at $[CO_2] : [CH_4] \approx 0.23$ (at 1600 K), the process in the post-flame zone can occur in such a mode that $K_t = ([CO_2][H_2])/([CO][H_2O]) \approx 0.33$, i.e., under the conditions of apparent equilibrium in the whole post-flame zone, although the running concentrations of the reaction products continue to change in time.

Carbon dioxide and steam reforming processes. Figure 7 shows the results of modeling the kinetics of steam and carbon dioxide reforming of methane at 1600 K under isothermal conditions using the plug flow reactor model.

As can be seen, carbon dioxide and steam reforming (DR and SMR) of methane at short residence times from 10^{-3} to ~ 10^{-2} s involves only methane pyrolysis with the successive formation of ethylene and acetylene. CO_2 and H_2O are not noticeably consumed in this period. Their appreciable consumption starts at the reaction time of $>10^{-2}$ s, when acetylene appears in the reaction mixture in an appreciable concentration. At ~80% methane conversion, the acetylene concentration reaches a maximum and then decreases. In [19], we compared the methane conversion kinetics in steam and carbon dioxide reforming of methane with that in thermal pyrolysis; as we showed, in all the cases under consideration the methane conversion occurs similarly within the same time. Acetylene along with hydrogen is the major primary product. In steam and carbon dioxide reforming, the variation of the concentrations of water and carbon dioxide, respectively, occurs with a noticeable delay relative to the variation of the methane concentration; i.e., their active conversion starts already after accumulation of H radicals in the system.

In carbon dioxide reforming of methane, the hydrogen formed by methane pyrolysis can enter into the reverse water gas shift reaction (1):

$$H_2 + CO_2 \rightarrow CO + H_2O,$$

and, because of high concentrations of CO_2 and H_2 in the initial step of the process, $K_t = ([CO_2][H_2])/([CO][H_2O]) > K_{eq}$ (Fig. 8, DR region). With the progress of methane conversion, the CO_2 concentration decreases, the CO and H_2O concentrations increase, and K_t tends to K_{eq}.

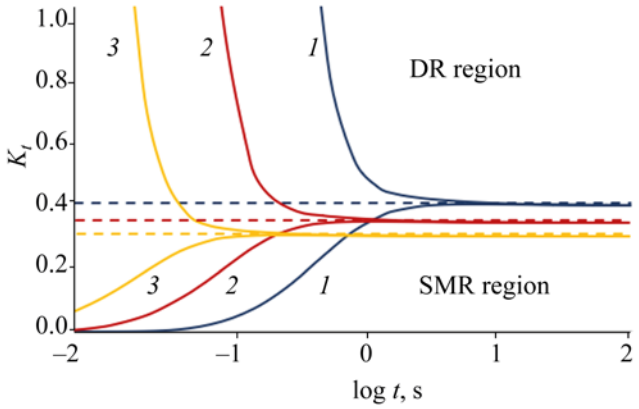

Fig. 8. Variation of the quantity $K_t = ([CO_2][H_2])/([CO][H_2O])$ in the course of carbon dioxide (DR) and steam (SMR) conversion of methane at (*1*) 1700, (*2*) 1600, and (*3*) 1500 K.

A decrease in the CO_2 concentration is also due to the reaction with acetylene, occurring simultaneously with the reverse reaction of the steam reforming of CO. As a result, the running value of K_t in the intermediate step of the conversion reaches K_{eq}, and further conversion of CO_2 and acetylene occurs at the running values of K_t corresponding to the equilibrium value, K_{eq}.

In steam reforming of methane, the initial value of K_t is close to zero. Owing to an increase in the H_2 concentration and to the reaction between H_2O and CO formed by steam reforming of acetylene, $K_t = ([CO_2][H_2])/([CO][H_2O])$ starts to increase (Fig. 8, SMR region), and the running value of K_t in the intermediate step of the conversion reaches K'_{eq}. Further conversion of H_2O and acetylene occurs at the running values of K_t close to K_{eq}.

Of course, assignment of the revealed process features to steam reforming of CO is formal, because the reacting system contains a large amount of various radicals effecting diverse reactions, but the above-noted processes characteristic of WGSR can prevail.

CONCLUSIONS

The non-catalytic processes of the partial oxidation of methane and its steam and carbon dioxide reforming, as well as the steam reforming of CO, are reactions involving three elements, C, H, and O, and the equilibrium gas mixtures formed by the conversion at 1400–1800 K can contain as major products only H_2, CO, H_2O, and CO_2. Their distribution corresponds to the equilibrium constant K_{eq} of the steam reforming of CO. At the preset initial content of C, H, and O, the equilibrium yield of each of the above-noted four products is determined by a system of four equations, of which three equations are balance equations with respect to each element (C, H, O), and the fourth equation is the expression $K'_{eq} = ([H_2]_{eq}[CO_2]_{eq})/([CO]_{eq}[H_2O]_{eq}) = K_{eq}$.

At certain initial C : H : O ratio and process conditions, solid carbon C_{solid} can also appear in the system as an equilibrium product.

The kinetic curves characterizing the forward and reverse reactions of the steam reforming of CO are characterized by an induction period, which can be considerably reduced by introducing definite compounds. Non-catalytic processes of the partial oxidation and the steam and carbon dioxide reforming of methane start at H_2, CO, H_2O, and CO_2 concentrations far from their equilibrium values, so that $K_t = ([CO_2][H_2])/([CO][H_2O]) < K_{eq}$ for partial oxidation and steam reforming of methane, whereas $K_t = ([CO_2][H_2])/([CO][H_2O]) > K_{eq}$ for carbon dioxide reforming of methane. In this step of the process, elementary reactions characteristic of the forward and reverse reactions of steam reforming of CO can play a significant role. Then, when the process is still far from completion, the running value of K_t reaches $K'_{eq} \approx K_{eq}$, and further conversion of the unchanged CH_4 and acetylene occurs at running values of K_t close to K_{eq}.

AUTHOR INFORMATION

V.I. Savchenko, ORCID: https://orcid.org/0000-0001-9823-6844

Ya.S. Zimin, ORCID: https://orcid.org/0000-0002-3645-9361

E. Busillo, ORCID: https://orcid.org/0000-0002-3456-0351

A.V. Nikitin, ORCID: https://orcid.org/0000-0002-8236-3854

I.V. Sedov, ORCID: https://orcid.org/0000-0001-9648-4895

V.S. Arutyunov, ORCID: https://orcid.org/0000-0003-0339-0297

FUNDING

Studies were performed within the framework of the Program of Basic Research of State Academies of Sciences, theme nos. 0089-2019-0018 (Institute of Problems of Chemical Physics, Russian Academy of Sciences, state registry no. AAAA-A19-119022690098-3) and 0082-2019-0014

(Federal Research Center of Chemical Physics, Russian Academy of Sciences, state registry no. AAAA-A20-120020590084-9).

CONFLICT OF INTEREST

I.V. Sedov is the acting Deputy Editor-in-Chief of Neftekhimiya/Petroleum Chemistry journal. Other authors declare no conflict of interest requiring disclosure in this article.

OPEN ACCESS

REFERENCES

1. Haber, F. and Richard, F., *Z. Anorg. Allg. Chem.*, 1904, vol. 38, pp. 5–64. https://doi.org/10.1002/zaac.19040380103
2. Ashok Jangam, Sonali Das, Dewangan, N., Plaifa Hongmanorom, P., Wai Ming Hui, and Sibudjing Kawi, *Catal. Today*, 2020, vol. 358, pp. 3–29. https://doi.org/10.1016/j.cattod.2019.08.049
3. Byron Smith, R.J., Muruganandam, L., and Murthy Shekhar Shantha, *Int. J. Chem. Reactor Eng.*, 2010, vol. 8, no. 1. https://doi.org/10.2202/1542-6580.2238
4. Trusov, B.G., *Proc. XIV Int. Symp. on Chemical Thermodynamics*, 2002, p. 483.
5. Healy, D., Kalitan, D.M., Aul, C.J., Petersen, E.L., Bourque, G., and Curran, H.J., *Energy Fuel*, 2010, vol. 24, no. 3, pp. 1521–1528. https://doi.org/10.1021/ef9011005
6. *NUI Galway*. Combustion Chemistry Center. Mechanism Downloads. (addressed December, 21, 2020). http://c3.nuigalway.ie/combustionchemistrycentre/mechanismdownloads/
7. Zhang, Q., Wang, J.F., and Wang, T.F., *Ind. Eng. Chem. Res.*, 2017, vol. 56, pp. 5174–5184. https://doi.org/10.1021/acs.iecr.7b00406
8. Arutyunov, V., Troshin, K., Nikitin, A., Belyaev, A., Arutyunov, A., Kiryushin, A., and Strekova, L., *Chem. Eng J.*, 2020, vol. 381, article 122706. https://doi.org/10.1016/j.cej.2019.122706
9. *Chemical WorkBench 4.1*. Kintech Lab Ltd. (addressed September 21, 2021). http://www.kintechlab.com
10. Savchenko, V.I., Nikitin, A.V., Zimin, Y.S., Ozerskii, A.V., Sedov, I.V., and Arutyunov, V.S., *Chem. Eng. Res. Des.*, 2021, vol. 175, no. 11, pp. 250–258. https://doi.org/10.1016/j.cherd.2021.09.009
11. Savchenko, V.I., Zimin, Y.S., Nikitin, A.V., Sedov, I.V., and Arutyunov, V.S., *J. CO_2 Util.*, 2021, vol. 47, no. 5, article 101490. https://doi.org/10.1016/j.jcou.2021.101490
12. Savchenko, V.I., Shapovalova, O.V., Nikitin, A.V., Arutyunov, V.S., and Sedov, I.V., *Russ. J. Appl. Chem.*, 2018, vol. 91, no. 9, pp. 1500−1512. https://doi.org/10.1134/S1070427218090136
13. Savchenko, V.I., Zimin, Y.S., Nikitin, A.V., Sedov, I.V., and Arutyunov, V.S., *Petrol. Chem.*, 2021, vol. 61, pp. 762–772. https://doi.org/10.1134/S0965544121070021
14. LeValley, T.L., Richard, A.R., and Fan, M., *Int. J. Hydrogen Energy*, 2014, vol. 39, pp. 16983–17000. https://doi.org/10.1016/j.ijhydene.2014.08.041
15. Bustamante, F., Enick, R.M., Killmeyer, R.P., Howard, B.H., Rothenberger, K.S., Cugini, A.V., Morreale, B.D., and Ciocco, M.V., *AIChE J.*, 2005, vol. 51, pp. 1440–1454. https://doi.org/10.1002/aic.10396
16. Bustamante, F., Enick, R.M., Cugini, A.V., Killmeyer, R.P., Howard, B.H., Rothenberger, K.S., Ciocco, M.V., Morreale, B.D., Chattopadhyay, S., and Shi, S., *AIChE J.*, 2004, vol. 50, pp. 1028–1041. https://doi.org/10.1002/aic.10099
17. Bradford, B.W., *J. Chem. Soc.*, 1933, pp. 1557–1563.
18. Savchenko, V.I., Nikitin, A.V., Sedov, I.V., Ozerskii, A.V., and Arutyunov, V.S., *Chem. Eng. Sci.*, 2019, vol. 207, pp. 744–751. https://doi.org/10.1016/j.ces.2019.07.012
19. Busillo, E., Savchenko, V.I., and Arutyunov, V.S., *Petrol. Chem.*, 2021, vol. 61, pp. 1–5. https://doi.org/10.1134/S0965544121110037